Polyoxometalate Surfactants as Unique Molecules for Interfacial Self- Assembly

5 AUTHORS, INCLUDING:

Juan Giner-Casares
CIC biomaGUNE
46 PUBLICATIONS **283** CITATIONS

SEE PROFILE

Sebastian Polarz
Universität Konstanz
110 PUBLICATIONS **2,680** CITATIONS

SEE PROFILE

Helmuth Moehwald
Max Planck Institute of Colloids and Interfaces
1,004 PUBLICATIONS **38,630** CITATIONS

SEE PROFILE

Polyoxometalate Surfactants as Unique Molecules for Interfacial Self-Assembly

Juan J. Giner-Casares,*,[†,‡] Gerald Brezesinski,[†] Helmuth Möhwald,[†] Steve Landsmann,[§] and Sebastian Polarz*,[§]

[†]Department of Interfaces, Max Planck Institute of Colloids and Interfaces, Science Park Golm, 14476 Potsdam, Germany
[‡]Department of Physical Chemistry, University of Córdoba, Campus de Rabanales, 14014 Córdoba, Spain
[§]Department of Chemistry, University of Konstanz, D-78457 Konstanz, Germany

Ⓢ *Supporting Information*

ABSTRACT: Whereas, commonly, Langmuir monolayers are structurally dominated by the aliphatic chains, we present here the first case of monolayers where the chains merely serve anchoring at the air/water interface and the organization is dictated by the hydrophilic head group self-assembling in a hexagonal lattice. These head groups are polyoxometalates known for their multifunctional potential. The chain length has been systematically varied, allowing for a general study of the impact of the chain length on the supramolecular structure. These model structures are studied here by a combination of modern techniques, the leading ones being X-ray reflectivity and grazing incidence X-ray diffraction. The quantitative structural insights offered in this Letter might represent a starting point for the rational design and study of a new class of emulsions, including an organic tail and a multifunctional inorganic polar head.
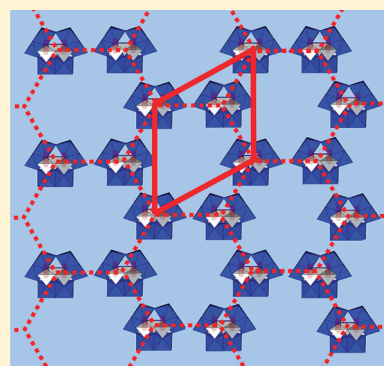
SECTION: Surfaces, Interfaces, Catalysis

The hierarchical organization of materials on multiple length scales represents one of the key steps toward the emergence of advanced properties. The formation of supramolecular aggregates by self-assembly processes is one of the most valuable tools for structuring.[1] As the design of supramolecular structures is expanded, more complex architectures are reached. In order to improve the reproducibility and simplicity in experimental procedures, a decrease of the number of required building blocks is highly desirable.

Surfactants occupy a leading position in interfacial self-assembly, with fundamental relevance in many areas from biology to nanotechnology.[2] Polyoxometalates (POMs) are molecular metal oxo clusters, with molybdates and tungstenates as the most prominent examples.[3] POMs and their supramolecular assemblies are materials of high relevance due to their performance in catalysis,[4] nonlinear optics,[5] energy storage,[6] magnetism,[7,8] and medicine.[9,10] POMs-containing 3D supramolecular structures have been achieved in bulk media, often with organic connectors between POM units,[11−14] as well as by POM derivatives with amphiphilic character.[15] The nano- and microstructures arise mainly from centrosymmetrical structures.[16,17] The assembly of POM units into 2D supramolecular structures has been performed by using an interfacial platform,[18] including at least one extra component, either as a connector or as a template, for example, surfactants.[19−22] Cronin and Liu have reported on the formation of nonordered Langmuir monolayers by dumb-shell-shaped POM−organic hybrids.[23] Chambers et al. reported

Langmuir monolayers of the POMs surfactants. However, no quantitative structural insights on the supramolecular arrangement was given, and no systematic study on the effect of the chain length on the structure was performed.[24] This is, on the other hand, needed to derive general rules on supramolecular assembly in the case on the interplay of the ordering in hydrophobic and hydrophilic sublayers. A general statement concerning the most adequate chain length for the POM surfactants is of high interest.

A standard surfactant is a molecular unit including a hydrophilic head group and a hydrophobic tail, usually hydrocarbon chains. Mechanistic studies concerning the detailed structures in the self-assembled structures are hampered by the inherent difficulties regarding the arrangement of the often less ordered head group. Traditionally, there has been a rather small electron density contrast between the polar head and aliphatic tail of the standard surfactant molecules.[2] The tremendous contrast for scattering studies characteristic of the new POM surfactants presented herein makes reflectivity experiments a first powerful experimental proof of a new concept in scattering studies, in which the polar head can be clearly distinguished from the aliphatic chains thanks to the large electron contrast. The contrast between the head and tail is much larger than any reported up to now for a

true surfactant. Moreover, the first experimental evidence of ordered polar head groups leading to a diffraction pattern is presented.

The quantitative structural data presented herein might represent a starting point for the design and study of a new class of emulsions, including an organic tail and a multifunctional inorganic polar head. Given that the feasibility of functional catalytic emulsions by these POM surfactants has been already proven,[25] the inorganic/organic assemblies that can be readily built using these POM surfactants are of maximum interest for both the new functionalities and physical insights to be attained. Thus, we expect these results to be of interest for further research concerning the structure and functionality of 3D assemblies of POM surfactants. Is it noteworthy that given the applications of the POMs in catalysis,[26] combined with the possibility of obtaining micelles of the POM surfactants following an easy and scalable procedure, these inorganic/organic assemblies of the POM surfactants are most promising for large-scale applications. Moreover, in a recent example, a nanometric inorganic/organic composite containing a bioactive antiviral POM unit was successfully carried to the inner region of cells, thereby proving the high interest of nanocomposites containing POMs as a new emerging approach in nanomedicine.[27]

The POM surfactants[24,25] are used as a single component for interfacial self-assembly. The surfactants contain the water-soluble POM cluster $[PW_{11}O_{39}]^{3-}$. The POM unit is covalently bound to two saturated hydrocarbon chains at exclusively one side of the POM unit. The new POM surfactants resemble the molecular structure of a classical surfactant, with a net dipolar moment. The POM surfactants possess the chemical formula $[PW_{11}O_{39}(SiC_nH_{2n+1})_2]Na_3$, named POM-$C_n$; n denotes the number of methylene units in each alkyl chain. The length of the hydrocarbon chain has been varied from C_{12} to C_{22} in order to systematically study the influence of the chain length on the supramolecular structure. Given the large difference in electron density between the hydrophilic head and the hydrophobic chains, the POM surfactants constitute a meaningful model for the study of the order of surfactants by X-ray.

The air/water interface is used for the self-assembly of the POM surfactants, the main advantage being the possibility of precise control of the area. The lateral interactions between molecules at the interface can be manipulated and measured precisely. The air/water interface has been used for assembling of different materials of interest, for example, nanoparticles.[28,29] The new POM surfactants are highly suitable for the formation of Langmuir monolayers (see Scheme 1). The high level of detail in the molecular structure can be exclusively attained by the different in situ experimental techniques used in combination with the Langmuir technique.

The feasibility of building stable Langmuir monolayers of POM surfactants is assured by their surface pressure–molecular area (π–A) isotherms (see Figure 1). The isotherms show good reproducibility (see Supporting Information, Figure S1). The monolayers are stable up to a surface pressure of ~30 mN/m. See Supporting Information, Figure S2 for isobaric creep measurements. The exception is the Langmuir monolayer formed by the POM-C_{12}, which collapses at a lower surface pressure of ~15 mN/m. The main reason for this collapse appears to be a reduced chain length, which results in a reduction of the magnitude on the hydrophobic interactions that anchor the surfactants at the air/water interface.

Scheme 1. (Top) Top-View of the Air/Water Interface Covered with a Langmuir Monolayer of the POM-C_n; (Bottom) Side-View of a Monolayer of the POM-C_n at the Air/Water Interface
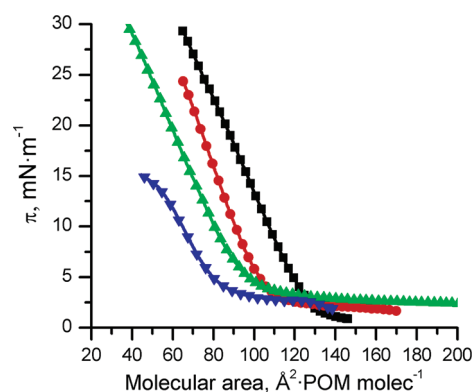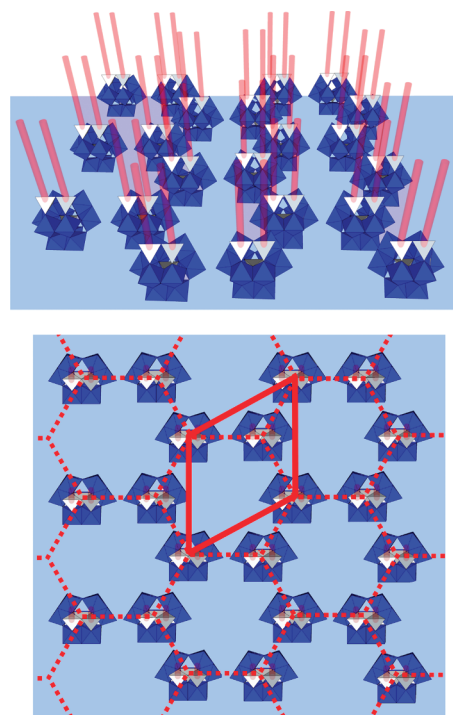

Figure 1. Surface pressure–molecular area (π–A) isotherms of the POM-C_n surfactants. (Black ■) POM-C_{22}. (Red ●) POM-C_{18}. (Green ▲) POM-C_{16}. (Blue ▼) POM-C_{12}.

By extrapolating the condensed section of the π–A isotherms to zero surface pressure, the limiting area per molecule in the Langmuir monolayer can be estimated.[30] From the π–A isotherms, these are, approximately, 130, 110, 100, and <90 Å^2 per POM-C_{22}, POM-C_{18}, POM-C_{16}, and POM-C_{12}, respectively. A decreasing limiting area with decreasing chain length is observed. For the monolayer of POM-C_{22}, the limiting molecular area agrees with the expected area for a POM molecule, 130 Å^2. Therefore, the POM-C_{22} molecules are assumed not to be solubilized in the water subphase. Given that the POM moiety is water-soluble, partial formation of micelles is expected, provoking loss of material from the air/water interface into bulk water. Indeed, micelle formation by the POM surfactants has been reported.[25] In this scenario, desorption of the POM surfactant molecules with decreasing

chain length is favored, as observed in the experiments. In other words, the longer the chain, the more stable the monolayer as the hydrophobic interactions between hydrocarbon chains stabilize the Langmuir monolayer. Note that the POM-C_{12} monolayer is not stable at the air/water interface over a long span of time. However, the time required for losing 50% of the material into the subphase is slightly more than 1 h. Although this period of time might be regarded as short concerning the long-term stability, 1 h was enough to perform the described experiments, including the surface pressure−molecular area isotherm shown in Figure 1.

The formation of a single monolayer at the air/water interface is proved by in situ X-ray reflectivity[31,32] yielding the electron density profiles for the different POM monolayers, also given in Figure 2 for the POM-C_{18}. Given that the POM
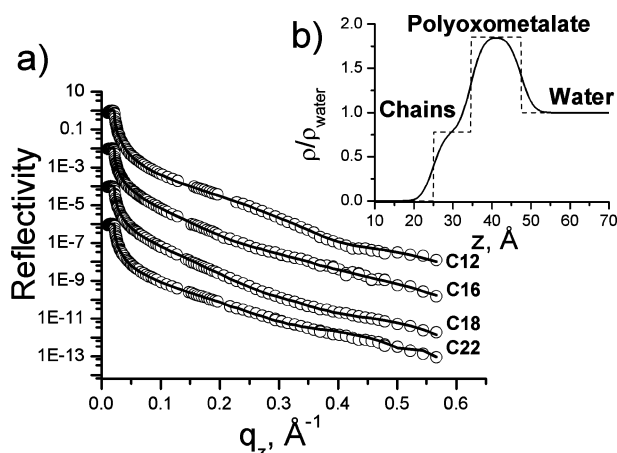

Figure 2. (a) Experimental X-ray reflectivity curves for the POM-C_n monolayers (open circles) at 20 mN/m and the corresponding fit (solid line). POM-C12 data were acquired at 15 mN/m. Each curve has been offset vertically for clarity. (b) Electron density profile of the POM-C_{18} monolayer at 20 mN/m.

units can be considered hard objects on a surface, it is fundamental to prove the formation of a true monolayer instead of a macroscopic glassy material on the air/water interface. There are no relevant differences in the electron density profiles for the different POM Langmuir monolayers. The electron density fitting boxes for the different POM surfactants are shown in Table S1 (Supporting Information). The electron density is noted as defined as ρ. A relative electron density is used, using the electron density of the water subphase as unity, ρ/ρ_{water}. The electron density curves are similar for all cases, fitting into two boxes. The first box includes the POM head, and the second box includes the hydrocarbon chains. The latter exhibits an electron density of $\rho/\rho_{water} \ll 1$, typical for disordered alkanes. The normalized electron density of the POM head ρ/ρ_{water} is ~1.9, a value significantly larger than expected for the polar head of a regular surfactant, usually ~1.3. The strong reflectivity signal is expected, given the large electron density of the POM groups, which contain W atoms. The electron density profile proves the existence of a well-defined single monolayer at the air/water interface, therefore discarding the formation of multilayers. The large difference in the electron density between the heads and the tails enables these new POM surfactants to be useful models for studying the interfacial behavior. In this sense, the effect on polar head ordering by chemical modification of either the hydrocarbon

tails or the POMs head or insertion of alkanes as cosurfactants is expected to be easily accessed by experiments. Moreover, any effect of molecules or ions that are present at the subphase on the ordering of the polar heads might also be analyzed. Further analysis of the ordering of the POM head is discussed below.

Besides the collapse of POM-C_{12} at a lower surface pressure, there are no relevant differences in the shape of the $\pi-A$ isotherms of the POM surfactants. The $\pi-A$ isotherms show a value of surface pressure greater than 0, ~2 mN/m, even at large values of molecular areas, except for the POM-C_{22} monolayer. The nonzero values of surface pressure could indicate the formation of aggregates of POM-C_n molecules. The occurrence of aggregates of POM-C_n at the expanded state of the monolayer might be based in the self-aggregation tendency of the POM head group units. The homogeneity at the micrometer level of the POM Langmuir monolayer has been checked by Brewster angle microscopy (BAM), showing only homogeneous monolayers (Supporting Information, Figure S4) for the whole range of molecular areas and the stability experiments. In the case of occurrence of POM-C_n aggregates, the aggregates should be smaller in diameter than the lateral resolution of our BAM instrument, 2 μm. However, there is no direct experimental proof of the existence of such aggregates. Given the significant solubility of water of the POM-C_n molecules, a certain contribution from the Gibbs adsorption process might be expected as well. In further research concerning the fabrication of devices with the transferred films of POM surfactants, AFM imaging would be of high relevance for studying the actual morphology of the transferred films.

The slope of the isotherms does not show any significant change for the complete range of surface pressure, indicating the absence of a phase transition along the isotherms. The physical state of the hydrocarbon chains has been examined in situ by infrared reflection absorption spectrometry (IRRAS) (see Supporting Infortmation, Figures S2 and S3). The symmetric $\nu_s(CH_2)$ and antisymmetric $\nu_{as}(CH_2)$ stretching vibrational modes can be used to monitor the aggregation state of the hydrocarbon chains.[33] The $\nu_s(CH_2)$ and $\nu_{as}(CH_2)$ bands are located at ~2853 and ~2922 cm^{-1}, respectively, indicating a disordered state, consistent with the X-ray reflectivity data.

One of the most remarkable features of the Langmuir monolayer methodology is the possibility of inducing molecular ordering at the air/water interface. An unambiguous proof of crystalline ordering at the air/water interface is given by in situ synchrotron radiation-based grazing incidence X-ray diffraction (GIXD).[34] The GIXD technique is exclusively sensitive to ordered structures at the interface. The crystalline structures at the air/water interface give rise to Bragg peaks. The Bragg peaks display a characteristic value of Q_{xy} and Q_z and are expressed in the reciprocal space in Å^{-1}. The POM polar heads display a well-defined molecular ordering at the air/water interface, as shown by the GIXD peaks in Figure 3. To the best of our knowledge, there is no previous report on polar head ordering in Langmuir monolayers that gives rise to a GIXD signal, that is, a diffraction pattern due to crystalline ordering. Here, there is apparently the unique situation of an ordered head group.

The POM surfactant monolayers exhibit Bragg peaks at Q_{xy} of ~0.45 Å^{-1} and Q_z of ~0.17 Å^{-1} (see Figure 3). The position of the Bragg peaks is dependent on neither the chain length nor the surface pressure applied. We attribute the persistence of the crystalline structure to the existence of a disordered region of
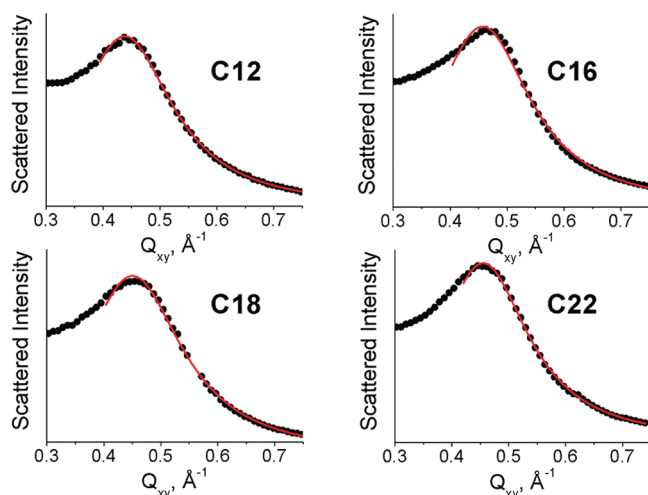
Figure 3. Bragg peaks for the POM-C_n surfactants, POM-C_{22}, POM-C_{18}, POM-C_{16}, and POM-C_{12}. (Black symbols) GIXD data. (Red line) Fitting for the proposed model. The surface pressure was 20 mN/m, except for POM-C_{12}, with a surface pressure of 10 mN/m.

POM molecules, which increase the degree of packing with the compression of the monolayer. Therefore, the position of the GIXD peaks is not modified upon compression of the POM-C_n monolayer, while the mean area per POM molecule is reduced, as shown in Figure 1. In other words, by confining the POM moieties at the air/water interface, a self-assembly of the POM heads into a 2D crystalline structure is obtained. The main driving force for this self-assembly is the lateral interaction between POM units, as demonstrated by the formation of a 2D well-defined nanometric structure. The formation of the supramolecular structure takes place regardless of the chain length of the POM surfactant. The crystalline parameters are shown in Table 1. Given the occurrence of one Bragg peak and

Table 1. Primitive Unit Cell Parameters, In-Plane Q_{xy} and Out-of-Plane Q_z Components of the Scattering Vector, and Projection of POM Moieties in the xy Plane (A_{xy}) of the POM-C_n Monolayers at $T = 21°C^a$

C_n	A, Å^b	Q_{xy}, Å^{-1}	Q_z, Å^{-1}	A_{xy}, Å^2	L, nm
C_{12}	16.564	0.438 (0.206)	0.148 (0.464)	237.6	1.22
C_{16}	15.876	0.457 (0.206)	0.127 (0.467)	218.3	1.21
C_{18}	15.738	0.461 (0.209)	0.192 (0.431)	214.5	1.31
C_{22}	15.945	0.455 (0.195)	0.167 (0.472)	220.2	1.20

^{a}The fwhm of the peaks is given in parentheses. L is the calculated thickness by the fwhm of the Bragg rods. $^b a = b$.

considering previous results for Langmuir monolayers, a hexagonal arrangement with an empty center of the POM units is assumed. The red line in Figure 3 shows the fitting of the GIXD data to this model. The POM head might be described by a sphere with a diameter of ~1.3 nm. A limiting area of ~1.33 nm^2 is expected for the POM head. Given the unit cell distance, an area per POM molecule of ~1.2 nm^2 is obtained; this value agrees with the expected area and the value obtained by the isotherms (Figure 1).[35] The in-plane coherence length is approximately $L_{xy} \approx 0.9(2\pi)/\text{fwhm}(Q_{xy})$. Thus, a L_{xy} of ~2.8 nm is obtained, corresponding to two POM units, as expected for an empty hexagonal packing. The thickness of the monolayer (L) can be estimated from the full width at half-maximum (fwhm) of the Bragg rods by using the equation $L \approx$ $0.9(2\pi)/\text{fwhm}(Q_z)$.[36] The values of thicknesses are shown in Table 1, revealing complete agreement with the thicknesses obtained by X-ray reflectivity for the POM head, ~1.3 nm. This value agrees with the value expected from geometrical considerations of the POM head.

In conclusion, using a new class of POM-based surfactants, a 2D supramolecular structure including POM groups has been built at the air/water interface. The self-assembly of the POM units is mainly driven by the lateral interactions between POM moieties. This is the first clear example of ordering of molecules at the air/water interface dictated by packing of the hydrophilic head groups rather than the hydrophobic tails. The lattice of the head groups could be measured and described convincingly. The self-assembly of the POMs has been performed by using a single component, with neither organic connectors nor templates required. A relevant contribution arising from tail ordering is absent in the POM-C_n monolayers. This is understandable because the area demand of two stretched chains is only about 20% of that of the head groups. It may be tempting in future experiments to fill the left space by alkanes, which might induce chain order to study the competition between head and tail ordering. The approach presented herein offers valuable insights for a rationale design of new inorganic–organic hybrids that self-assemble at interfaces efficiently, with no required extra components. Because the POM head groups also exhibit a high application potential, it will be intriguing in future experiments to manipulate their ordering to advance understanding of the interactions as well as the consequences for electrical and optical properties.

■ ASSOCIATED CONTENT

Ⓢ Supporting Information
Experimental procedures, reproducibility of the isotherms, isobaric creep measurements, electron density parameters, IRRAS spectra and maximum wavenumbers, and Brewster angle microscopy images. This material is available free of charge via the Internet at http://pubs.acs.org.

■ AUTHOR INFORMATION

Corresponding Author
*E-mail: jjginer@uco.es (J.J.G.-C.); sebastian.polarz@uni-konstanz.de (S.P.).

■ ACKNOWLEDGMENTS

■ REFERENCES

(1) Lehn, J.-M. Perspectives in Supramolecular Chemistry — From Molecular Recognition Towards Molecular Information-Processing and Self-Organization. *Angew. Chem., Int. Ed.* **1990**, *29*, 1304–1319.

(2) Evans, D. F.; Wennerström, H. *The Colloidal Domain: Where Physics, Chemistry, Biology, and Technology Meet*, 2nd ed.; Wiley-VCH: New York, 1999.

(3) Pope, M. T.; Mueller, A. Polyoxometalate Chemistry: An Old Field with New Dimensions in Several Disciplines. *Angew. Chem., Int. Ed.* **1991**, *30*, 34–48.

(4) Corma, A.; García, H.; Llabrés i Xamena, F. X. Engineering MOF for catalysis. *Chem. Rev.* **2010**, *110*, 4606–4655.

(5) Liu, C.-G.; Guan, W.; Yan, L.-K.; Su, Z.-M.; Song, P.; Wang, E.-B. Second-Order Nonlinear Optical Properties of Transition-Metal-Trisubstituted Polyoxometalate-Diphosphate Complexes: A Donor-Conjugated Bridge-Acceptor Paradigm for Totally Inorganic Non-linear Optical Materials. *J. Phys. Chem. C* **2009**, *113*, 19672–6.

(6) Kishore, P. S.; Viswanathan, B.; Varadarajan, T. K. Acid Based Carbon Supported Noble Metal Electrodes for Energy Conversion Application. *J. Phys. Chem. C* **2009**, *113*, 12918–12925.

(7) Coronado, E.; Gómez-García, C. Polyoxometalate-Based Molecular Materials. *Chem. Rev.* **1998**, *98*, 273–296.

(8) Lehmann, J.; Gaita-Ariño, A.; Coronado, E.; Loss, D. Spin Qubits with Electrically Gated Polyoxometalate Molecules. *Nat. Nanotechnol.* **2007**, *2*, 312–317.

(9) Rhule, J., T.; Hill, C. L.; Judd, D. A.; Schinazi, R. F. Polyoxometalates in Medicine. *Chem. Rev.* **1998**, *98*, 327–357.

(10) Geng, J.; Li, M.; Wang, E.; Qu, X. Polyoxometalates as Inhibitors of the Aggregation of Amyloid β Peptides Associated with Alzheimer's Disease. *Angew. Chem., Int. Ed.* **2011**, *50*, 4184–4188.

(11) Lin, X.; Li, W.; Zhang, J.; Sun, H.; Yan, Y.; Wu, L. Thermotropic LC of a Non-Mesogenic Group Surfactant Encapsulated POMs Complexes. *Langmuir* **2010**, *26*, 13201–13209.

(12) Zheng, S.-T.; Zhang, J.; Li, X.-X.; Fang, W.-H.; Yang, G.-Y. Cubic POM–Organic Molecular Cage. *J. Am. Chem. Soc.* **2010**, *132*, 15102–15103.

(13) Coronado, E.; Clemente-León, M.; Galán-Mascarós, J. R.; Giménez-Saiz, C.; Gómez-García, C. J.; Martínez-Ferrero, E. Design of Molecular Materials Combining Magnetic, Electrical and Optical Properties. *J. Chem. Soc., Dalton Trans.* **2000**, *21*, 3955–3961.

(14) Yin, S.; Li, W.; Wang, J.; Wu, L. Mesomorphic Structures of Protonated Surfactant-Encapsulated Polyoxometalate Complexes. *J. Phys. Chem. B* **2008**, *112*, 3983–3988.

(15) Polarz, S.; Smarsly, B.; Antonietti, M. Colloidal Organization and Clusters: Self-Assembly of Polyoxometalate–Surfactant Complexes towards Three-Dimensional Organized Structures. *ChemPhysChem* **2001**, *2*, 457–461.

(16) Zhang, J.; Song, Y.-F.; Cronin, L.; Liu, T. Self-Assembly of Organic–Inorganic Hybrid Amphiphilic Surfactants with Large Polyoxometalates as Polar Head Groups. *J. Am. Chem. Soc.* **2008**, *130*, 14408–14409.

(17) Fan, D. W.; Hao, J. C. Magnetic Aligned Vesicles. *J. Colloid Interface Sci.* **2010**, *342*, 43–48.

(18) Xu, B.; Xu, L.; Gao, G.; Guo, W.; Liu, S. Effects of Film Structure on Electrochromic Properties of the Multilayer Films Containing Polyoxometalates. *J. Colloid Interface Sci.* **2009**, *330*, 408–414.

(19) Coronado, E.; Mingotaud, C. Hybrid Organic/Inorganic Langmuir–Blodgett Films. A Supramolecular Approach to Ultrathin Magnetic Films. *Adv. Mater.* **1999**, *11*, 869–872.

(20) Clemente-León, M.; Coronado, E.; Gómez-García, C.; Mingotaud, C.; Ravaine, S.; Romualdo-Torres, G.; Delhaes, P. Polyoxometalate Monolayers in Langmuir–Blodgett Films. *Chem.—Eur. J.* **2005**, *11*, 3979–3987.

(21) Clemente-León, M.; Agricole, B.; Mingotaud, C.; Gómez-García, C.; Coronado, E.; Delhaes, P. Toward New Organic/Inorganic Superlattices: Keggin Polyoxometalates in Langmuir and Langmuir–Blodgett Films. *Langmuir* **1997**, *13*, 2340–2347.

(22) Bao, Y.-Y.; Bi, L.-H.; Wu, L.-X.; Mal, S. S.; Kortz, U. Preparation and Characterization of Langmuir–Blodgett Films of Wheel-Shaped Cu-20 Tungstophosphate and DODA by Two Different Strategies. *Langmuir* **2000**, *25*, 13000–13006.

(23) Misdrashi, M. F.; Wang, M.; Pradeep, C. P.; Li, F.-Y.; Lydon, C.; Xu, L.; Cronin, L.; Liu, T. Amphiphilic Properties of Dumbbell-Shaped Inorganic–Organic–Inorganic Molecular Hybrid Materials in Solution and at an Interface. *Langmuir* **2011**, *27*, 9193–9202.

(24) Chambers, R. C.; Atkinson, E. J. O.; McAdams, D.; Hayden, E. J.; Brown, D. J. A. Creating Monolayers and Thin Films of a Novel Bis(alkyl) Substituted Asymmetrical Polyoxotungstate, {[CH₃(CH₂)₁₁Si]₂OSiW₁₁O₃₉}⁴⁻ Using the Langmuir–Blodgett Technique. *Chem. Commun.* **2003**, 2456–2457.

(25) Landsmann, S.; Lizandara-Pueyo, C.; Polarz, S. A New Class of Surfactants with Multinuclear, Inorganic Head Groups. *J. Am. Chem. Soc.* **2010**, *132*, 5315–5321.

(26) Okuhara, T. Water-Tolerant Solid Acid Catalysts. *Chem. Rev.* **2002**, *102*, 3641–3666.

(27) Geisberger, G.; Paulus, S.; Gyenge, E. B.; Maake, C.; Patzke, G. R. Targeted Delivery of Polyoxometalate Nanocomposites. *Small* **2011**, *7*, 2808–2814.

(28) Stefaniu, C.; Chanana, M.; Wang, D.; Novikov, D. V.; Brezesinski, G.; Möhwald, H. Biocompatible Magnetite Nanoparticles Trapped at the Air/Water Interface. *ChemPhysChem* **2010**, *11*, 3585–3588.

(29) Dong, A.; Chen, J.; Vora, P. M.; Kikkawa, J. M.; Murray, C. B. Binary NPs Films at Air/Water Interface Binary Nanocrystal Superlattice Membranes Self-Assembled at the Liquid–Air Interface. *Nature* **2010**, *466*, 474–477.

(30) Gaines, G. *Insoluble Monolayers at Liquid–Gas Interfaces*; Wiley-Interscience: New York, 1966.

(31) Kjaer, K.; Als-Nielsen, J.; Helm, C. A.; Tippman-Krayer, P.; Möhwald, H. Synchrotron X-ray-Diffraction and Reflection Studies of Arachidic Acid Monolayers at the Air–Water Interface. *J. Phys. Chem.* **1989**, *93*, 3200–3206.

(32) Helm, C. A.; Möhwald, H.; Kjaer, K.; Als-Nielsen, J. Phospholipid Monolayer Density Distribution Perpendicular to the Water-Surface — A Synchrotron X-Ray Reflectivity Study. *Europhys. Lett.* **1987**, *4*, 697–703.

(33) Mendelsohn, R.; Brauner, J. W.; Gericke, A. External Infrared Reflection–Absorption Spectrometry Monolayer Films at the Air–Water Interface. *Annu. Rev. Phys. Chem.* **1995**, *46*, 305–334.

(34) Kaganer, V. M.; Möhwald, H.; Dutta, P. Structure and Phase Transitions in Langmuir Monolayers. *Rev. Mod. Phys.* **1999**, *71*, 779–819.

(35) Hinrichsen, E. L.; Feder, J.; Jossang, T. Random Packing of Disks in Two Dimensions. *Phys. Rev. A* **1990**, *41*, 4199–4209.

(36) Daillant, J.; Alba, M. High-Resolution X-ray Scattering Measurements: I. Surfaces. *Rep. Prog. Phys.* **2000**, *63*, 1725–1777.